

Enhancement of electroluminescence properties of red diketopyrrolopyrrole-doped copolymers by oxadiazole and carbazole units as pendants

Yi Jin^a, Yanbin Xu^a, Zhi Qiao^a, Junbiao Peng^b, Baozheng Wang^b, Derong Cao^{a,*}

^aSchool of Chemistry and Chemical Engineering, South China University of Technology, Guangzhou 510640, China

^bInstitute of Polymer Optoelectronic Materials and Devices, South China University of Technology, Guangzhou 510640, China

ARTICLE INFO

Article history:

Received 18 June 2010

Received in revised form

5 September 2010

Accepted 16 September 2010

Available online 1 October 2010

Keywords:

Diketopyrrolopyrrole

Conjugated polymer

Light-emitting diodes (LED)

ABSTRACT

Two novel diketopyrrolopyrrole (DPP)-based copolymers **P1**–**2** were prepared by doping red emitting DPP monomer (1 mol%) into benzothiadiazole, alkoxybenzene and 9,9-dialkylfluorene-based copolymers through base-free Suzuki polymerization. **P1** contained the pendants of electron-transport oxadiazole and hole-transport carbazole, but **P2** did not contain them. **P1** had higher glass transition temperature than **P2**. The electroluminescence (EL) devices of **P1** and **P2** (ITO/PEDOT:PSS/polymer/CsF/Al) exhibited red emission with external quantum efficiency of 0.63% and 0.18%, and with brightness of 2681 and 885 cd/m², respectively. The results show that the EL properties of **P1** are much better than that of **P2** due to the introduction of oxadiazole and carbazole as the pendants. The pendants could restrain aggregation which might induce fluorescence quenching and are of benefit to keep high charge mobility. The efficient energy transfer existed among the pendants, polymer backbone and DPP unit. These factors should be responsible for the higher EL performance of **P1**.

© 2010 Elsevier Ltd. All rights reserved.

1. Introduction

Diketopyrrolopyrrole (DPP) derivatives are a class of strongly fluorescent heterocyclic pigments and their structures could be easily optimized through variations of substituents at the 2,5- and 3,6-positions [1–3]. However, high content of DPP unit in the DPP-based conjugated polymer decrease the quantum yield in solid state and the electroluminescence (EL) efficiency of the polymeric light-emitting diodes (PLED) [4,5]. The EL performance is enhanced by doping low content of DPP unit (guest) in the main chain of polyfluorene (host) but emission wavelength is blue shifted [4].

In the dopant/host system, carrier trapping and subsequent direct carrier recombination on the guest molecule can adjust charge balance in emitting layer and enhance the device efficiencies [6–10]. Besides this positive effect, charge trapping can lower carrier mobility and often cause a high operating voltage [11–15], even disturb the original charge balance and decrease the EL performance [4,12,15]. This negative effect can be addressed by using of a blend of carrier transport material with EL polymer [13]. The unavoidable drawback of the approach is the possible phase separation between two different kinds of materials, which reduces the lifetime and stability of the devices [16,17].

In solid state, luminogenic molecules lie in close vicinity and incline to form aggregates. Chromophore aggregation could usually quench the emission of organic luminophores which have very high luminescence efficiencies in the dilute solutions, due to formation of detrimental species such as excimers [18–21]. This effect can be mitigated by covalently attaching branched chains, bulky cyclics, spiro kinks, and dendritic wedges to aromatic rings [22]. Moreover, balanced charge injection and mobility and high charge mobility are desirable to move the charge recombination zone away from the near electrodes and improve the exciton generation rate in high efficient electroluminescent devices [6,23,24]. However, in conjugated polymers, charge transport occurs via on-chain migration and interchain hopping of carriers between adjacent chains which is the rate limiting step. The interchain charge transport can occur at only where there is sufficient overlap of wave functions between polymer chains. The bulky substituent should hinder the interchain interaction and chain movement. As a result, charge mobility of the polymer with bulky pendant is lower than one without bulky pendant [25–27]. This negative effect can be overcome by grafting oxadiazole and carbazole units as pendants into conjugated polymers, because these substituents have good charge conduction property [23,24,28–30]. That is to say, the grafted copolymers could facilitate charge transport and injection, decrease operating voltage, and enhance maximum brightness and EL efficiency in the emitting diodes [16,30–35]. Furthermore, by incorporating benzothiadiazole (BT) and dioctyloxybenzene into the fluorene polymer, the resulting

* Corresponding author. Tel./fax: +86 20 87110245.

E-mail address: drcao@scut.edu.cn (D. Cao).

copolymers possess high electron and hole transporting properties and high EL performance [36].

In this paper, low content of red emitting DPP monomer (1 mol%) was doped into the main chain of benzothiadiazole and alkoxybenzene-based polyfluorene through Suzuki polymerization to obtain high efficient red emitting polymer. Oxadiazole as the electron-transport moiety, and *N*-carbazolyl as the hole-transport moiety were introduced to the copolymers as pendants, in order to restrain aggregation induced fluorescence quenching and the negative impact of dopant, to obtain balanced charge injection and mobility, and lower operating voltage. The photophysical, electrochemical and electroluminescence properties of the polymers were evaluated and compared with the polymer without the pendants as well as with the polymer without the dopant.

2. Experimental

2.1. Instrumentation and materials

NMR (^1H and ^{13}C) spectra were collected on a Bruker DRX 400 spectrometer (in CDCl_3 or $\text{DMSO}-d_6$, TMS as internal standard). APCI-MS spectra were recorded with a Bruker Esquire HCT plus mass spectrometer. Elemental analysis was performed using a Vario EL III instrument. Fourier transform infrared (FT-IR) spectra were recorded on an RFX-65A (Analect Co.) spectrometer. The number-average molecular weight (M_n) and weight-average molecular weights (M_w) were determined by Waters GPC 515–410 in tetrahydrofuran (THF) with a calibration curve of polystyrene standards. Ultraviolet–visible (UV–vis) absorption spectra were recorded on an HP 4803 instrument. Cyclic voltammetry (CV) was carried out on an EG&G model 283 computer-controlled potential/galvanostat (Princeton Applied Research) with platinum electrodes at a scanning rate of 50 mV/s against a calomel reference electrode with a nitrogen-saturated solution of 0.1 M tetrabutyl ammonium hexafluorophosphate (Bu_4NPF_6) in acetonitrile. Thermogravimetric analysis (TGA) was conducted on a Pyris 1 TGA under a heating rate of 10 °C/min and a N_2 flow rate of 20 mL/min. Differential scanning calorimetry (DSC) measurement was performed on a Diamond DSC under N_2 at a heating rate of 10 °C/min. PL and EL spectra were recorded on an Instaspec IV CCD spectrophotometer (Oriol Co.). The current–luminance voltage (I – L – V) was measured using a Keithley 236 source measurement unit and a calibrated silicon photodiode. The luminance was calibrated using a PR-705 Spectra Scan spectrophotometer (Photo research).

4-Hydroxybenzo hydrazide [37], 2,5-dioctyl-3,6-bis(4'-formylphenyl)pyrrolo[3,4-c]pyrrole-1,4-dione [38], 1,4-dibromo-2,5-bis(octyloxy)benzene [39], 4,7-dibromo-2,1,3-benzothiadiazole [40], 9,9-bis(*N*-carbazolyl-hexyl)-2,7-dibromofluorene [41], 2,7-dibromo-9,9-dioctyl fluorine [42] were synthesized according to the published literature; other chemicals were obtained from commercially available resources.

2.2. 1,4-Dibromo-2,5-bis(6-bromohexyloxy)benzene (3)

A mixture of hydroquinone (5.416 g, 49 mmol), NaOH (4.328 g, 108.2 mmol) and ethanol (105 ml) was added dropwise into the solution of 1,6-dibromohexane (60 g, 245 mmol) and ethanol (75 ml) at 90 °C. After refluxing for 4 h, the mixture was extracted with CH_2Cl_2 and the residue was removed. The solution was washed with H_2O and the solvent was evaporated under reduced pressure. To oily product ethanol (200 ml) was added that gave precipitates of 1,4-bis(6-bromohexyloxy)benzene (**2**) as white solid (9.43 g, yield = 44%), mp: 87–90 °C. The product was used directly for the next step without further purification. A mixture of Br_2 (9.632 g, 60 mmol) and CH_2Cl_2 (15 ml) was added dropwise into the solution of **2** (10.5 g,

24 mmol) in CH_2Cl_2 (50 ml) at 0 °C. The mixture was stirred for 4 h at 0 °C followed by stirring for 14 h at room temperature. After that NaHSO_3 aqueous solution was added into the mixture until brown color disappeared. The mixture was extracted with CH_2Cl_2 , washed with water and dried over MgSO_4 . After filtration, the solvent was evaporated under reduced pressure and the residue was recrystallized with CH_2Cl_2 and ethanol to give **3** as white solid (12.207 g, yield = 86%). mp: 90–91 °C. ^1H NMR (400 MHz, CDCl_3 , δ , ppm): 7.09 (s, 2H, Ar), 3.96 (t, J = 6.4 Hz, 4H, CH_2), 3.43 (t, J = 6.8 Hz, 4H, CH_2), 1.92–1.89 (m, 4H, CH_2), 1.84–1.81 (m, 4H, CH_2), 1.54–1.51 (m, 8H, CH_2).

2.3. 4-tert-Butyl-*N'*-(4-hydroxybenzoyl)benzohydrazide (6)

A solution of DMF (100 ml), pyridine (20.8 g, 263 mmol) and 4-tert-butylbenzoyl chloride (25.78 g, 131 mmol) was added dropwise to the solution of 4-hydroxybenzo hydrazide (20 g, 131 mmol) and DMF (450 ml) at 0 °C. The mixture was stirred at 0 °C for 4 h. It was poured into water and washed with water. The crude product was redissolved in NaOH aqueous solution. After filtration, the red solution was neutralized with HCl to give **6** as white solid (25.87 g, yield = 63.1%). mp: 258–260 °C. ^1H NMR (400 MHz, $\text{DMSO}-d_6$, δ , ppm): 10.33 (s, 1H, OH), 10.22 (s, 1H, NH), 10.12 (s, 1H, NH), 7.84 (d, J = 8 Hz, 2H, Ar), 7.79 (d, J = 8 Hz, 2H, Ar), 7.52 (d, J = 8 Hz, 2H, Ar), 6.83 (d, J = 8 Hz, 2H, Ar), 1.30 (s, 9H, CH_3).

2.4. 4-(5-(4-tert-Butylphenyl)-1,3,4-oxadiazol-2-yl)phenol (7)

A mixture of **6** (21.107 g, 67.5 mmol), pyridine (1.069 g, 13.5 mmol) and SOCl_2 (215 ml) was stirred at 88 °C for 6 h. The solvent was removed and the residue was poured into ice water. After filtration, filter cake was recrystallized with ethanol to give **7** as white solid (14.371 g, yield = 72.3%). mp: 240–242 °C. ^1H NMR (400 MHz, $\text{DMSO}-d_6$, δ , ppm): 10.36 (s, 1H, OH), 8.00 (d, J = 8 Hz, 2H, Ar), 7.94 (d, J = 8 Hz, 2H, Ar), 7.62 (d, J = 8 Hz, 2H, Ar), 6.97 (d, J = 8 Hz, 2H, Ar), 1.31 (s, 9H, CH_3).

2.5. 2-(4-(6-(5-Bromo-4-(6-(4-(5-(4-(2-bromopropan-2-yl)phenyl)-1,3,4-oxadiazol-2-yl)phenoxy)hexyloxy)-2-methylphenoxy)hexyloxy)phenyl)-5-(4-tert-butylphenyl)-1,3,4-oxadiazole (8)

A mixture of **3** (7.06 g, 11.9 mmol), **7** (7.0 g, 23.8 mmol), NaOH (1.07 g, 26.2 mmol), tetrabutyl ammonium bromide (1.50 g, 4.65 mmol), DMSO (70 ml) and ethanol (70 ml) was heated to 90 °C for 6 h. After that the mixture was poured into water (500 ml) and precipitates were separated. These precipitates were washed with water then ethanol followed by recrystallization with CH_2Cl_2 and ethanol to give **8** as white solid (12.14 g, yield = 73.2%). mp: 169–172 °C. ^1H NMR (400 MHz, $\text{DMSO}-d_6$, δ , ppm): 8.06–8.02 (m, 8H, Ar), 7.52 (d, J = 8.4 Hz, 4H, Ar), 7.07 (s, 2H, Ar), 7.00 (d, J = 8.8 Hz, 4H, Ar), 4.04 (t, J = 6.4 Hz, 4H, CH_2), 3.96 (t, J = 6.4 Hz, 4H, CH_2), 1.85–1.84 (m, 8H, CH_2), 1.58–1.56 (m, 8H, CH_2), 1.35 (s, 18H, CH_3); ^{13}C NMR (100 MHz, CDCl_3 , δ , ppm): 161.9, 155.2, 150.0, 128.7, 126.7, 126.0, 121.1, 118.5, 116.2, 115.0, 111.1, 70.0, 68.0, 35.1, 31.1, 29.0, 25.7, 25.7; MS (APCI) calcd for $\text{C}_{54}\text{H}_{60}\text{Br}_2\text{N}_4\text{O}_6$ 1020.3, found 1021.3. Anal. Calc. for $\text{C}_{54}\text{H}_{60}\text{Br}_2\text{N}_4\text{O}_6$: C, 63.53; H, 5.92; N, 5.49. Found: C, 63.69; H, 6.15; N, 5.46.

2.6. 2,5-Dioctyl-3,6-bis{4'-[2-(4-bromophenyl)-2-cyano-vinyl]-phenyl}pyrrolo[3,4-c] pyrrole-1,4-dione (11)

A mixture of 2-(4-bromophenyl)acetonitrile (122 mg, 0.625 mmol), 2,5-dioctyl-3,6-bis(4'-formylphenyl)pyrrolo[3,4-c]pyrrole-1,4-dione (142 mg, 0.25 mmol) and potassium carbonate (863 mg,

6.25 mmol) in absolute ethanol (4 ml) was refluxed for 2.5 h. After cooling, the mixture was poured into H₂O (5 ml) and washed with water. Precipitates were separated and recrystallized with CH₂Cl₂ and methanol which gave **11** as red solid (100 mg, yield = 43%). mp: 263–264 °C. ¹H NMR (400 MHz, CDCl₃, δ, ppm): 7.96 (d, *J* = 8.0 Hz, 4H, Ar), 7.87 (d, *J* = 8.0 Hz, 4H, Ar), 7.52–7.47 (m, 10 H, Ar and CH = C), 3.76 (t, *J* = 7.2 Hz, 4H, NCH₂), 1.52 (m, 4H, CH₂), 1.17 (m, 20H, CH₂), 0.81 (t, *J* = 6.8 Hz, 6H, CH₃); ¹³C NMR (100 MHz, CDCl₃, δ, ppm): 162.4, 147.5, 140.6, 135.5, 132.8, 132.3, 129.8, 129.7, 129.4, 127.4, 124.0, 117.3, 111.8, 110.6, 41.9, 31.7, 29.4, 29.1, 29.0, 26.7, 22.6, 14.1; MS (APCI) calcd for C₅₂H₅₂N₄O₂Br₂ 924.2, found 925.7. Anal. Calc. for C₅₂H₅₂N₄O₂Br₂: C, 67.52; H, 5.67; N, 6.06. Found: C, 67.59; H, 5.70; N, 6.04.

2.7. Synthesis of P1

A mixture of **11** (9.3 mg, 0.01 mmol), **8** (168.4 mg, 0.163 mmol), 9,9-bis(*N*-carbazoyl-hexyl)-2,7-dibromofluorene (135.7 mg, 0.163 mmol), 4,7-dibromo-2,1,3-benzothiadiazole (48.5 mg, 0.163 mmol), 9,9-dihexylfluorene-2,7-bis(trimethyleneboronate) (258.9 mg, 0.500 mmol), tetrakis(triphenylphosphine)-palladium(0) (18.0 mg, 0.015 mmol), tetrabutyl ammonium fluoride (523 mg, 2.00 mmol)

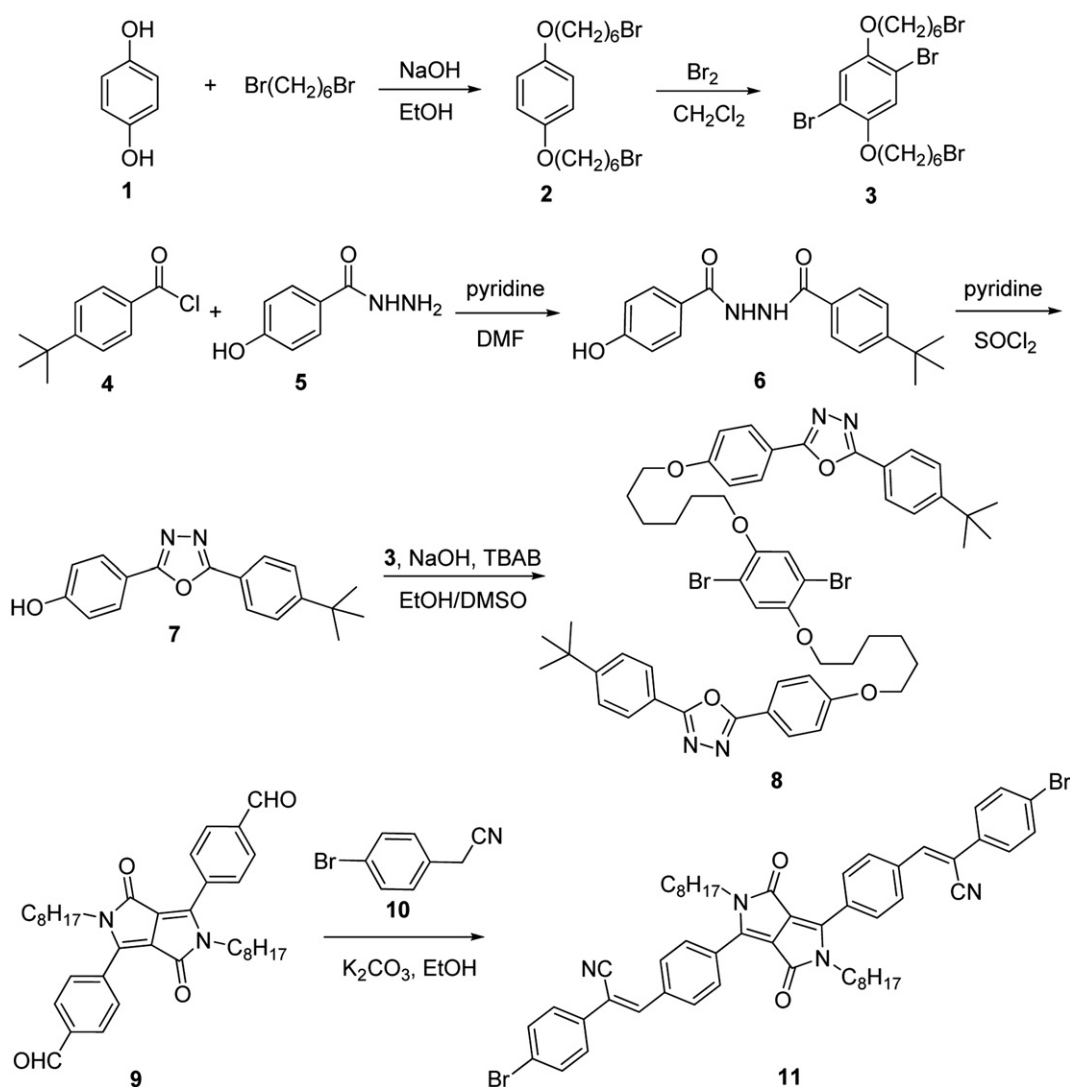
and anhydrous toluene (10 ml) was stirred at 120 °C for 60 h. 9,9-Dihexylfluorene-2,7-bis(trimethyleneboronate) (30.0 mg, 0.060 mmol) was added, and again stirred for 6 h. Bromobenzene (31.0 mg, 0.200 mmol) was added, and further stirred for 6 h. The mixture was cooled to room temperature, and washed with water. The organic layer was collected, and methanol was added. The precipitate was collected and dissolved in CHCl₃, and then acetone was added. The precipitate was collected and extracted with acetone in Soxhlet apparatus for 24 h to give **P1** as orange solid (349 mg, yield = 78%). FT-IR (film, cm⁻¹): 3051, 2928, 2856, 1612, 1495, 1462, 1377, 1256, 1013, 817, 749.

P0 was prepared as yellow solid (333 mg, yield = 75%) by using the same synthetic procedure of **P1**. FT-IR (film, cm⁻¹): 3051, 2928, 2856, 1613, 1495, 1459, 1377, 1255, 1013, 817, 750.

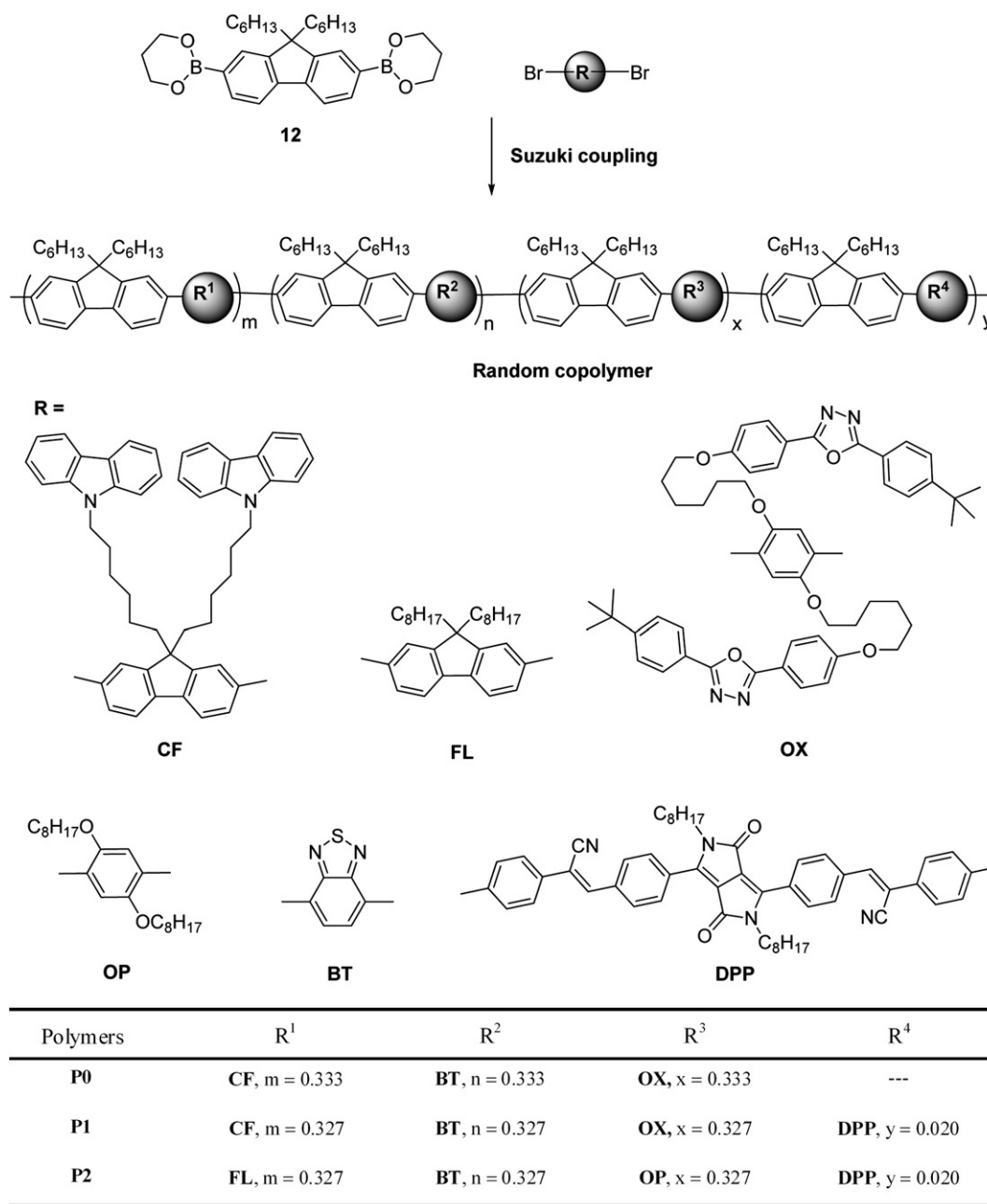
P2 was prepared as orange solid (176 mg, yield = 56%) by using the same synthetic procedure of **P1**. FT-IR (film, cm⁻¹): 2927, 2855, 1608, 1460, 1377, 1252, 816.

2.8. Light-emitting diode (LED) fabrication and characterization

The polymers were dissolved in toluene and THF and filtered through a 0.45-μm filter. Patterned indium tin oxide (ITO) coated



Scheme 1. Syntheses of monomers.



Scheme 2. Syntheses and composition of polymers.

glass substrates were cleaned with acetone, detergent, distilled water, and 2-propanol and subsequently in an ultrasonic bath. After treatment with oxygen plasma, 40 nm of poly(3,4-ethylenedioxythiophene) (PEDOT) doped with poly(styrenesulfonic acid)

Table 1
Structural, thermal, and photophysical data of the polymers.

Polymer	M_w	PDI	T_d (°C)	T_g (°C)	λ_{abs}^a (nm)	λ_{PL}^b (nm)
P0	25848	2.55	407	101	296, 370, 438 (296, 370, 457)	416, 438, 542 (546)
P1	28138	2.90	403	103	296, 370, 438 (296, 370, 457)	416, 438, 542 (544, 618)
P2	17296	2.08	412	85	370, 438 (370, 457)	416, 438, 542 (534, 626)

^a The absorption peaks in CHCl₃ and film (in brackets).

^b The PL emission peaks in CHCl₃ and film (in brackets).

(PSS; Batron-P 4083, Bayer AG) was spin-coated onto the ITO substrate, followed by drying in a vacuum oven. A thin film of the polymer was coated onto the anode via spin casting inside a dry box. The film thickness of the active layers was 80 nm, as measured with Alfa Step 500 surface profiler (Tencor). A thin layer of CsF (1.5 nm) and subsequently 120 nm layers of Al were vacuum-evaporated subsequently on the top of an EL polymer layer under a vacuum of 1×10^{-4} Pa.

3. Results and discussion

3.1. Synthesis and characterization

The synthetic route of the monomers and polymers are shown in Schemes 1 and 2. Anhydrous and base-free Suzuki polymerization [43] was used for preparation of the polymers to suppress the

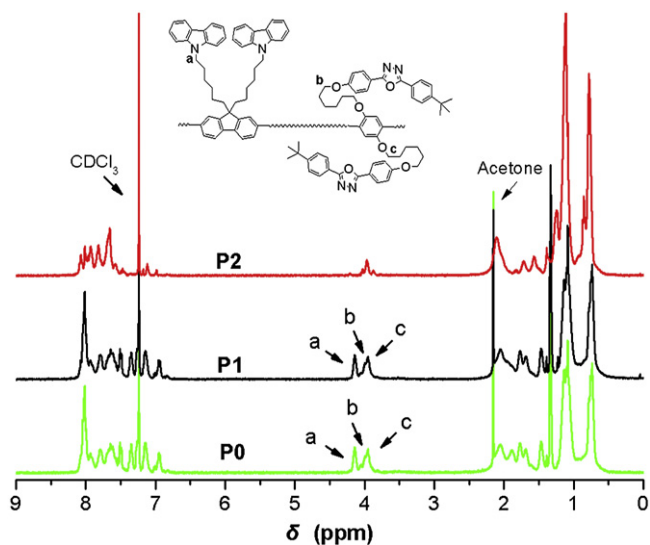


Fig. 1. ^1H NMR spectra of copolymers in CDCl_3 .

hydrolysis of amide configuration of DPP ring. The resulting copolymers could be readily dissolved in common organic solvents, such as chloroform, toluene, and THF. Their chemical structures were verified by ^1H NMR (Fig. 1) and FT-IR. Gel-permeation chromatography (GPC) analysis with polystyrene standards showed that these copolymers had weight-average molecular weights (M_w) of 28138–17296 with polydispersity indices (PDI, M_w/M_n) of 2.90–2.08 (Table 1). Decomposition temperatures of the polymers were almost similar, with 5% weight loss temperatures ranging from 403 to 412 $^\circ\text{C}$, which indicated their good thermal stability. Glass transition temperatures of **P0** and **P1** were 101 and 103 $^\circ\text{C}$, respectively. The values were higher than that of **P2** (85 $^\circ\text{C}$), showing that the introduction of oxadiazole and carbazole side chains could improve the morphological stability of the polymers.

3.2. Spectroscopic properties

P0 and **P1** had identical UV–Vis absorption spectra in CHCl_3 and film (Table 1). The absorptions at 370, 438 nm could be attributed to the polyfluorene part and benzothiadiazole part of the polymer, respectively. The absorption of DPP unit ($\lambda_{\text{max}} = 519$ nm) was not observed in the absorption spectra of the polymers (Fig. 2).

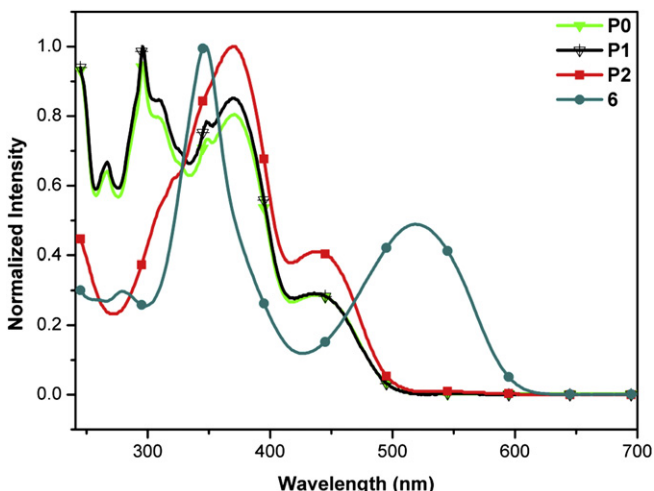


Fig. 2. Absorption spectra of DPP monomer and polymers in CHCl_3 .

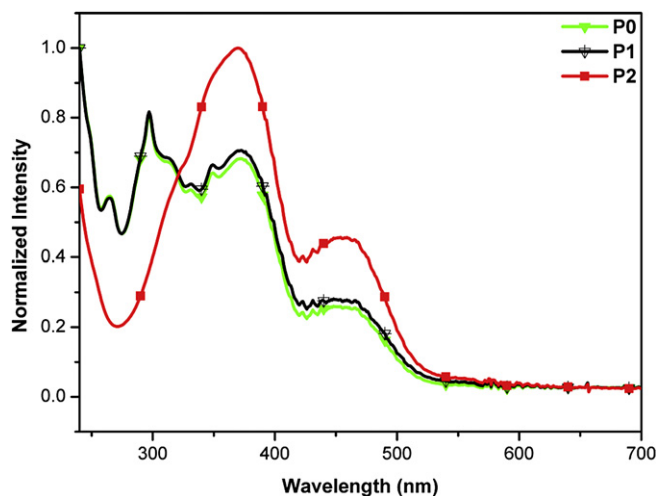


Fig. 3. Absorption spectra of polymers in film.

Moreover, all polymers showed broad absorption bands centered at 457 nm in film (Fig. 3).

The PL spectra of all polymers were similar and the emission band of DPP unit ($\lambda_{\text{em}} = 604$ nm) was hardly observed, due to the low DPP content in the dilute solution (Fig. 4). In contrast, the PL spectra of **P1** and **P2** in film exhibited a strong emission peak from DPP at 618 and 626 nm, respectively. The emission peak of polymer backbone became weak, indicating that energy transferred to the DPP unit via Förster energy transfer because of the efficient overlap of the absorption spectrum of DPP with PL spectrum of **P0** (Figs 2 and 5). The emission peak of the DPP unit was red shifted 8 nm from **P1** to **P2**. The reason for this might be that the carbazole and oxadiazole in the side chains of **P1** could more efficiently restrict π – π aggregation and intramolecular planarization of DPP than octyl of **P2** [22,34,35].

3.3. Electrochemical properties

Cyclic voltammetry measurements on drop-cast all polymers and DPP monomer films were conducted in acetonitrile with Bu_4NPF_6 as the electrolyte, calomel electrode as reference electrode. The HOMO and LUMO levels were determined from onset

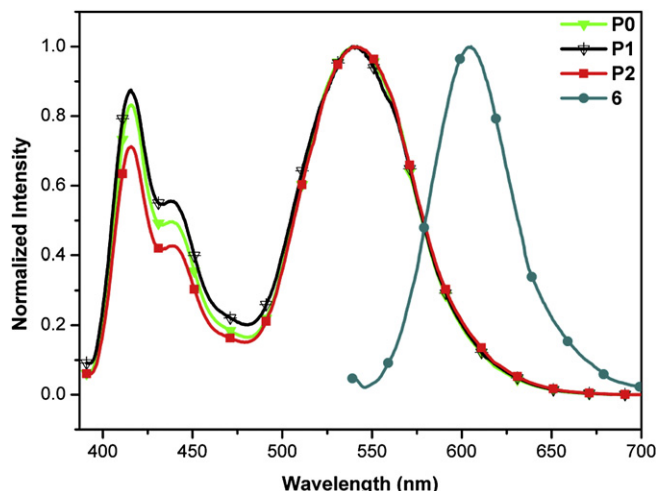


Fig. 4. PL spectra of DPP monomer and polymers in CHCl_3 .

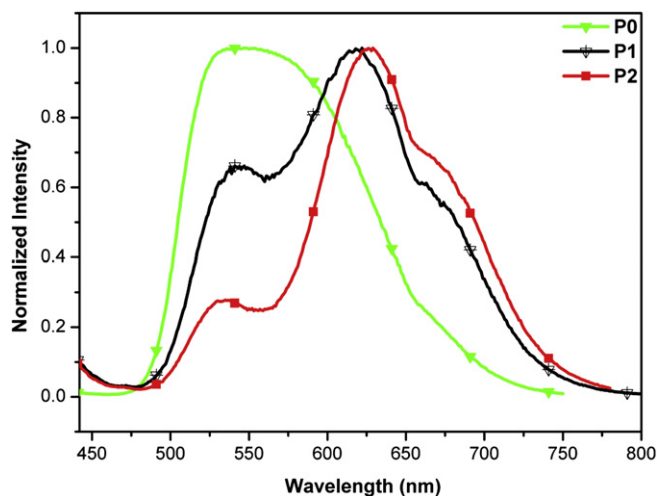


Fig. 5. PL spectra of polymers in film.

potential of first oxidation and reduction peak during anodic and cathodal sweep in the cyclic voltammetry measurements, respectively ($E_{HOMO} = -(E_{oxd} + 4.4)$ eV, $E_{LUMO} = -(E_{red} + 4.4)$ eV) [23]. As the 1,3,4-oxadiazole and carbazole units were introduced into copolymer, the HOMO energy level increased. The HOMO energy levels of **P0** and **P1** (−5.66 eV and −5.68) were closer to that of PEDOT:PSS (−5.2 eV) [44] than that of **P2** (−5.74 eV). This means that the hole-injection barriers for **P1** and **P0** decreased relative to **P2**. However, the LUMO levels of **P0**, **P1** and **P2** were similar. The HOMO and LUMO levels of DPP monomer (−5.58 and −3.57 eV) were above and below the corresponding values of **P0** (−5.66 and −3.44 eV), respectively. Considering the extended conjugated length of the DPP unit in conjugation with neighboring conjugated segments in the polymer backbone, the actual HOMO level of the DPP unit in the backbone should be above −5.58 eV and the actual LUMO level should be below −3.57 eV. This indicated possible charge trapping of the DPP unit in the electroluminescence process [45] (Table 2).

3.4. Electroluminescence properties

The EL spectra of polymers were collected at current density 12 mA/cm². The EL spectra of **P1** and **P2** exhibited a strong emission peak from DPP at 620 and 624 nm, respectively, while the EL emission **P0** at 548 nm was from polymer backbone (Fig. 6). The dramatic difference between the PL and EL spectra reveals that Förster energy transfer does not account solely for the observed EL. Another dominant mechanism for exciting DPP would be direct charge trapping at the dopant unit, followed by recombination with opposite charges [7–10] (Table 3).

The maximum luminance efficiency of the polymer LED with the configuration of ITO/PEDOT:PSS/**P1**/CsF/Al was 2.21 cd/A, while that of **P0** and **P2** were 5.86 and 0.29 cd/A, respectively. The CIE coordinates of **P1** and **P2** were (0.61, 0.37) and (0.64, 0.35) which

Table 2
Electrochemical Data of the Copolymers and DPP monomer.

Polymer/Monomer	E_{oxd}^a (V)	E_{red}^a (V)	HOMO ^b (eV)	LUMO ^b (eV)
P0	1.26	−0.96	−5.66	−3.44
P1	1.28	−0.96	−5.68	−3.44
P2	1.34	−0.93	−5.74	−3.47
6	1.18	−0.83	−5.58	−3.57

^a Onset potential vs calomel electrode.

^b Estimated from the onset potential.

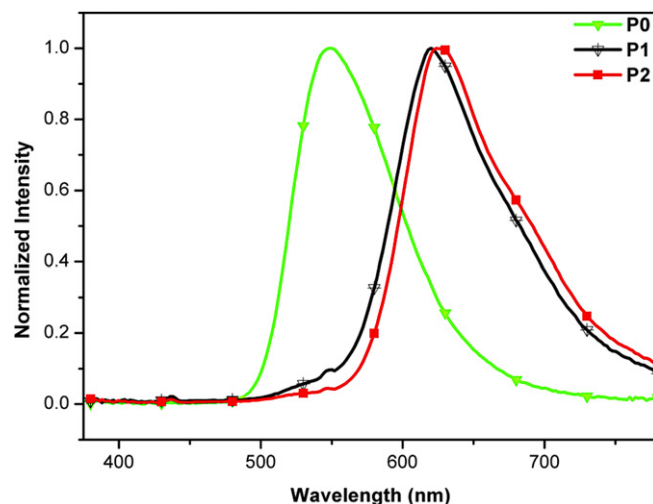


Fig. 6. EL spectra of polymers.

were close to the standard red (0.66, 0.34) demanded by the National Television System Committee. The maximum external quantum efficiency (EQE) of **P1** and **P2** were 0.63%, 0.18%, which were higher than that of the red emission polymer PF-DPP50 (EQE_{max} = 0.13%, CIE (0.62, 0.37)) [4]. The higher electroluminescence performance of **P1** might be due to several reasons. The bulky substituents of carbazole and oxadiazole could mitigate chromophore aggregation and restrict formation of detrimental species such as excimers [22,34,35]. The lower hole-injection barrier is of benefit to holes injection, which might be of benefit to balanced charge injection. Oxadiazole and carbazole substituents have good charge conduction property [23,24,29,30], which could facilitate charge transport. High charge mobility is desirable to move the charge recombination zone away from the near electrodes and improve the exciton generation rate in high efficient electroluminescent devices [6,23,24]. Carbazole group acted as a hole trapping site for efficient electron-hole recombination to yield blue-emitting excitons [46] and the energy could transfer to polymer backbone and then to DPP unit. Energy transfer also existed among oxadiazole, polymer backbone and DPP unit [33]. These factors could enhance EL performance.

Carbazole has high HOMO level which is of benefit to hole injection and good hole conduction property [30]. Oxadiazole has good electron mobility [24,28]. Thus grafting oxadiazole and carbazole units as pendants into conjugated polymers should enhance current density. However, the current density of **P1** was slightly lower than that of **P2** below 9.7 V.

During charge transport process of the conjugated polymer, charge carriers will move along the backbone and hop at only

Table 3
Performances of Double-Layer LED Devices (ITO/PEDOT:PSS/Polymer/CsF/Al).

Polymer	λ_{em} (nm) ^a	CIE (x, y) ^b	V_{on}^c (V)	LE_{max}^d (cd/A)	EQE (%)	B_{max}^e (cd/m ²)	V_{Bmax}^f (V)	CD_{Bmax}^g (mA/cm ²)
P0	548	(0.42, 0.56)	3.1	5.86	1.26	5940	8.0	227
P1	620	(0.61, 0.37)	5.0	2.21	0.63	2681	10.3	236
P2	624	(0.64, 0.35)	5.0	0.29	0.18	885	12.0	289

^a Emission maximum of EL spectrum.

^b Calculated from the EL spectrum.

^c Turn-on voltage (defined as the voltage required to give a luminance of 1 cd/m²).

^d Maximum luminous efficiency.

^e Maximum brightness.

^f Operating voltage at the maximum brightness.

^g Current density at maximum brightness.

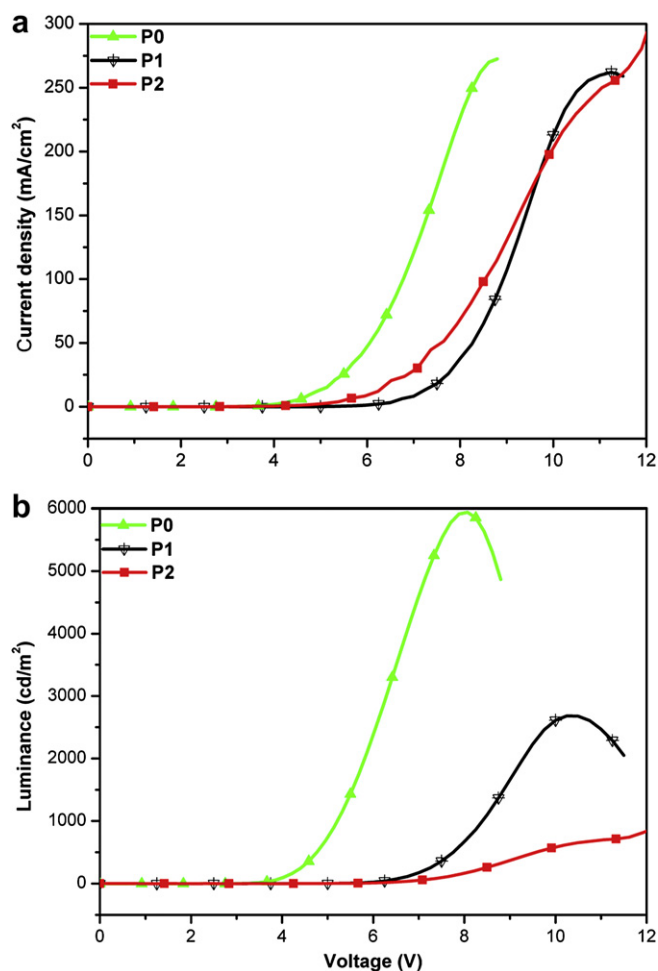


Fig. 7. (a) Current density–voltage (J – V), and (b) luminescence–voltage (L – V) characteristics of PLEDs of the polymers with the configuration of ITO/PEDOT:PSS/polymer/CsF/Al.

where two polymer chains are packed closely and form sufficient overlap of wave functions. Interchain hopping of carriers between adjacent chains is the rate limiting step. The bulky substituents of **P1** should restrict interchain interaction and chain movement and lower the mobility of carriers [25–27]. Furthermore, the incorporated carbazole pendant acted as a trap for the holes [46]. However, the high content (33 mol%) of carbazole in **P1** should be enough to open additional charge hopping channel among the carbazole units [12,47]. Moreover, the lower hole-injection barrier is of benefit to holes injection and oxadiazole group could enhance electron mobility [28,35]. These competition effects might be responsible for the comparable current density between **P1** and **P2**. The current density of **P1** increased more sharply with the enhanced voltage than that of **P2**. The possible reason is that the charge mobility of pendants might have larger dependence of the electric field than that for polymer backbone [48]. The driving voltage at 100 cd/m² was 3.9, 6.6, and 7.6 V for **P0**, **P1**, and **P2**, respectively (Fig. 7b).

EQE of the devices are displayed in Fig. 8. Although the initial quantum efficiency of **P0** and **P1** was higher than that of **P2**, the roll-off of the quantum efficiency for **P2** was much smaller than that of **P0** and **P1**. The quantum efficiency of **P2** was maintained almost the same with 0.17%–0.18% between 250 cd/m² and 885 cd/m² (EQE = 0.17% at 250 cd/m², 100 mA/cm²; EQE = 0.18% at 885 cd/m², 300 mA/cm²). In contrast, **P0** and **P1** exhibited

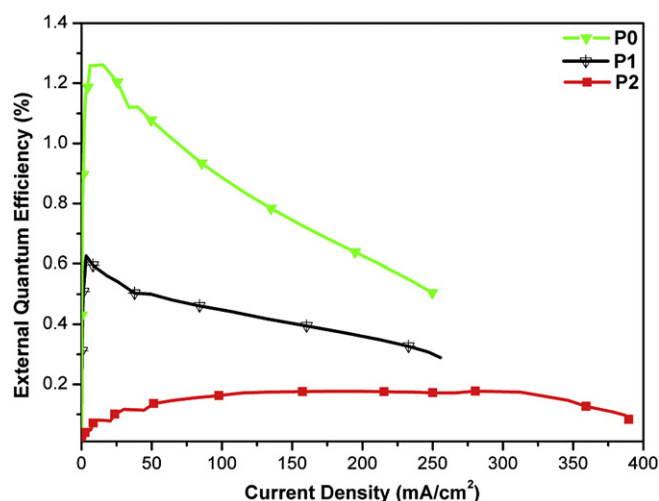


Fig. 8. EQE of OLEDs with the configuration of ITO/PEDOT:PSS/polymer/CsF/Al.

considerable reduction of efficiency with increasing current density. According to $\log \mu \propto \beta F^{1/2}$, where μ is the carrier mobility and F is the electric field strength [25,48], the hole and electron mobilities of **P0** and **P1** might be more different than that of **P2** in the high applied electric field. The recombination zone of carriers might extend to hole transporting layer or cathode with increasing current [49,50] and the degree of the extension was much larger in **P0** and **P1** than that in **P2**. Therefore, the sharp reduction of EL quantum efficiency in **P0** and **P1** might relate to the imbalanced electron and hole mobilities.

4. Conclusions

In conclusion, a series of benzothiadiazole, alkoxybenzene and fluorene-based copolymers were synthesized through base-free Suzuki polymerization. Introduction of oxadiazole and carbazole as the pendants enhanced glass transition temperature. The electrochemical measurements revealed that the pendants could affect electrochemical characteristics, and DPP unit and carbazole pendant could act as charge trapping sites in the polymers. The competition effects of restricted interchain carriers hopping, charge trapping, lower hole-injection barrier and enhanced charge mobility by oxadiazole and carbazole might be responsible for the comparable current density between **P1** and **P2**. The roll-off of the quantum efficiencies for **P1** and **P0** were much larger than that of **P2**, which might relate to the imbalanced electron and hole mobilities in the high applied electric field. The maximum luminances of **P0**, **P1**, and **P2** were 5940, 2681, and 885 cd/m² and the maximum EL efficiencies were 1.26%, 0.63%, and 0.18%, respectively. The CIE coordinates of **P1** and **P2** were (0.61, 0.37) and (0.64, 0.35) which were close to the standard red (0.66, 0.34) demanded by the National Television System Committee. **P1** possessed higher electroluminescence performance due to the introduction of oxadiazole and carbazole pendants compared to **P2**. The pendants could restrain aggregation which might induce fluorescence quenching and are of benefit to keep high charge mobility. The efficient energy transfer existed among the pendants, polymer backbone and DPP unit. These factors should be responsible for the higher EL performance of **P1**. It is worth mentioning that the EL quantum efficiency of **P1** was reduced in comparison to **P0**. The main reason may be a low quantum efficiency of DPP monomer which acts as a quench center for fluorescence. Structure modification of DPP monomers and optimization of EL devices should increase their EQE.

Acknowledgments

This work was supported by the National Natural Science Foundation of China (20872038), Science and Technology Planning Project of Guangdong Province, China (2007A010500011).

References

- [1] Rabindranath AR, Zhu Y, Heim I, Tieke B. *Macromolecules* 2006;39:8250–6.
- [2] Zhang K, Tieke B. *Macromolecules* 2008;41:7287–95.
- [3] Zhu Y, Rabindranath AR, Beylerlein T, Tieke B. *Macromolecules* 2007;40:6981–9.
- [4] Cao DR, Liu QL, Zeng WJ, Han SH, Peng JB, Liu SP. *Macromolecules* 2006;39:8347–55.
- [5] Qiao Z, Peng JB, Jin Y, Liu QL, Weng JN, Chen ZC, et al. *Polymer* 2010;51:1016–23.
- [6] Grimsdale AC, Chan KL, Martin RE, Jokisz PG, Holmes AB. *Chem Rev* 2009;109:897–1091.
- [7] Liu J, Cheng Y, Xie Z, Geng Y, Wang L, Jing X, Wang F. *Adv Mater* 2008;20:1357–62.
- [8] Liu J, Guo X, Bu L, Xie Z, Cheng Y, Geng Y, et al. *Adv Funct Mater* 2007;17:1917–25.
- [9] Liu J, Zhou Q, Cheng Y, Geng Y, Wang L, Ma D, et al. *Adv Funct Mater* 2006;16:957–65.
- [10] Tu G, Zhou Q, Cheng Y, Wang L, Ma D, Jing X, Wang F. *Appl Phys Lett* 2004;85:2172–4.
- [11] Pai DM, Yanus JF, Stolka M. *J Phys Chem* 1984;88:4714–7.
- [12] Campbell AJ, Bradley DDC, Virgili T, Lidzey DG, Antoniadis H. *Appl Phys Lett* 2001;79:3872–4.
- [13] Yang X, Neher D, Hertel D, Daeubler TK. *Adv Mater* 2004;16:161–6.
- [14] Tseng SR, Chen YS, Meng HF, Lai HC, Yeh CH, Horng SF, et al. *Synth Met* 2009;159:137–41.
- [15] Liu J, Tu GL, Zhou QG, Cheng YX, Geng YH, Wang LX, et al. *J Mater Chem* 2006;16:1431–8.
- [16] Jin SH, Kim MY, Kim JY, Lee K, Gal YS. *J Am Chem Soc* 2004;126:2474–80.
- [17] Xia Y, Friend RH. *Adv Mater* 2006;18:1371–6.
- [18] An BK, Kwon SK, Jung SD, Park SY. *J Am Chem Soc* 2002;124:14410–5.
- [19] Crenshaw BR, Weder C. *Chem Mater* 2003;15:4717–24.
- [20] Yuan CX, Tao XT, Ren Y, Li Y, Yang JX, Yu WT, et al. *J Phys Chem C* 2007;111:12811–6.
- [21] Zhao ZJ, Wang ZM, Lu P, Chan CYK, Liu DD, Lam JWY, et al. *Angew Chem Int Ed* 2009;48:7608–11.
- [22] Hong YN, Lam JWY, Tang BZ. *Chem Commun*; 2009:4332–53.
- [23] Kulkarni AP, Tonzola CJ, Babel A, Jenekhe SA. *Chem Mater* 2004;16:4556–73.
- [24] Huang J, Hou W-J, Li J-H, Li G, Yang Y. *Appl Phys Lett* 2006;89:133509–12.
- [25] Laquai F, Wegner G, Im C, Bassler H, Heun S. *J Appl Phys* 2006;99:023712–8.
- [26] Laquai F, Wegner G, Im C, Bassler H, Heun S. *J Appl Phys* 2006;99:033710–6.
- [27] Hoofman R, de Haas MP, Siebbeles LDA, Warman JM. *Nature* 1998;392:54–6.
- [28] Huang SP, Liao JL, Tseng HE, Jen TH, Liou JY, Chen SA. *Synth Met* 2006;156:949–53.
- [29] Xiang HF, Xu ZX, Roy VAL, Che CM, Lai PT, Zeng PJ, et al. *Appl Phys Lett* 2008;92:073305–7.
- [30] Yuan MC, Shih PI, Chien CH, Shu CF. *J Polym Sci Part A Polym Chem* 2007;45:2925–37.
- [31] Chen X, Liao J-L, Liang Y, Ahmed MO, Tseng H-E, Chen S-A. *J Am Chem Soc* 2003;125:636–7.
- [32] Jin Y, Song S, Kim JY, Kim H, Lee K, Suh H. *Thin Solid Films*; 2008:7373–80.
- [33] Wu CW, Tsai CM, Lin HC. *Macromolecules* 2006;39:4298–305.
- [34] Sung HH, Lin HC. *J Polym Sci Part A Polym Chem* 2005;43:2700–11.
- [35] Lee Y-Z, Chen X, Chen S-A, Wei P-K, Fann W-S. *J Am Chem Soc* 2001;123:2296–307.
- [36] Herguch P, Jiang XZ, Liu MS, Jen AKY. *Macromolecules* 2002;35:6094–100.
- [37] Peng YQ, Song GH. *Green Chem* 2001;3:302–4.
- [38] Qiao Z, Xu YB, Lin SM, Peng JB, Cao DR. *Synth Met* 2010;160:1544–50.
- [39] Wu CW, Lin HC. *Macromolecules* 2006;39:7985–97.
- [40] Ma Z, Lu S, Fan QL, Qing CY, Wang YY, Wang P, Huang W. *Polymer* 2006;47:7382–90.
- [41] Deng Y, Liu SJ, Fan QL, Fang C, Zhu R, Pu KY, et al. *Synth Met* 2007;157:813–22.
- [42] Grisorio R, Mastroianni P, Nobile CF, Romanazzi G, Suranna GP, Gigli G, et al. *Macromolecules* 2007;40:4865–73.
- [43] Brookins RN, Schanze KS, Reynolds JR. *Macromolecules* 2007;40:3524–6.
- [44] Yan H, Lee P, Armstrong NR, Graham A, Evmenenko GA, Dutta P, Marks TJ. *J Am Chem Soc* 2005;127:3172–83.
- [45] Zhen HY, Xu W, King W, Chen QL, Xu YH, Jiang JX, et al. *Macromol Rapid Commun* 2006;27:2095–100.
- [46] Liao JL, Chen X, Liu CY, Chen SA, Su CH. *J Phys Chem B* 2007;111:10379–85.
- [47] Laquai F, Hertel D. *Appl Phys Lett* 2007;90:142109–11.
- [48] Bettenhausen J, Stroehriegel P, Brutting W, Tokuhisa H, Tsutsui T. *J Appl Phys* 1997;82:4957–61.
- [49] Kang JW, Lee SH, Park HD, Jeong WI, Yoo KM, Park YS, Kim J. *J Appl Phys Lett* 2007;90:223508–10.
- [50] Giabink NC, Forrest SR. *Phys Rev B* 2008;77:235215–23.